FISEVIER

Contents lists available at ScienceDirect

Cement and Concrete Research

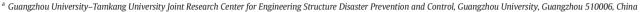
journal homepage: http://ees.elsevier.com/CEMCON/default.asp



CrossMark

The shrinkage of alkali activated fly ash

Y. Ma a,*, G. Ye b,c



- b Delft University of Technology, Faculty of Civil Engineering and Geosciences, Department of Materials and Environment, Delft, The Netherlands
- ^c Ghent University, Department of Structural Engineering, Ghent, Belgium

ARTICLE INFO

Article history: Received 23 April 2014 Accepted 27 October 2014 Available online 24 November 2014

Keywords: Alkali activated (D) Fly ash (D) Shrinkage (C) Pore size distribution (B)

ABSTRACT

In this study, the autogenous and drying shrinkage of alkali activated fly ash (AAFA) pastes prepared with different contents of sodium silicate solution are reported. A higher amount of both Na₂O and SiO₂ resulted in a larger autogenous and drying shrinkage. Although a large autogenous shrinkage was obtained during the first 1–3 days, cracking was not observed in the ellipse ring tests. In AAFA pastes, water was not a reactant, but mainly acted as a medium. The experiment results indicate that the autogenous shrinkage of AAFA is not caused by the well-known self-desiccation process that happened in cement paste, but related to the continuous reorganization and polymerization of the aluminosilicate gel structure. AAFA pastes with a larger drying shrinkage exhibited a higher weight loss. The different microstructures lead to the different drying shrinkage of these AAFA mixtures.

1. Introduction

The development of alkali activated materials (AAM) has been widely investigated [1–3] over the last few decades, mainly due to their environmental benefits [4] and superior engineering properties [5–7], e.g. the high early age strength under thermal curing (for the low-Ca system, e.g. alkali activated fly ash (AAFA)), and high resistance to chemical attack and high fire resistance. The industrial by-products, e.g. fly ash and blast furnace slag, and aqueous hydroxide or alkali silicate solutions are normally applied to produce alkali activated materials. Depending on the content of calcium in binders, the reaction products can be a three-dimensional aluminosilicate gel (for the low-Ca systems, e.g. alkali activated fly ash [8]), or a calcium silicate hydrate with a great degree of Al-participation, i.e. C–(A)–S–H gel (for the high-Ca systems, e.g. alkali activated slag (AAS) [9]).

The shrinkage of AAM is an important engineering property, influencing the cracking probability of AAM under the restrained condition. The previous studies [10,11] showed that the alkali activated slag had a significantly higher autogenous and drying shrinkage than the ordinary Portland cement (OPC). It was also reported that the activator species and dosage [11–13], particle size of slag [14] and curing conditions [15] were all important factors affecting the shrinkage of AAS. However, the investigations on the shrinkage, particularly the autogenous shrinkage of the alkali activated fly ash are limited. Some tests performed by Wallah and Rangan [16] and Fernández-Jiménez et al. [17] showed that the drying shrinkage of heat-cured AAFA mortar/concrete was much lower than OPC, while the drying shrinkage of AAFA samples cured under ambient conditions was significantly large. It indicates that

the drying shrinkage of AAFA is sensitive to the curing conditions. Further, the related mechanism of the shrinkage of AAFA is still not clear. For cement-based materials, the autogenous shrinkage is closely related to the chemical reaction, microstructure development and moisture conditions, i.e. internal relative humidity (RH), of the material. Given the completely different reaction mechanism and microstructure between AAFA and OPC [18–20], the autogenous shrinkage of AAFA should be very different from OPC. These uncertainties about the shrinkage of AAFA hamper the broader acceptance and application of this material in the construction industry.

The objective of this study is to provide a better understanding of the shrinkage mechanism of AAFA. The autogenous shrinkage and drying shrinkage of AAFA pastes prepared by sodium silicate solutions with different concentrations were investigated in this study. The factors influencing the shrinkage of AAFA pastes, including the internal RH, non-evaporable water content and pore structure were also explored. In addition, the ellipse ring tests were performed to assess the cracking potential of AAFA pastes under the restrained condition.

2. Materials and methods

2.1. Materials and mixture proportions of AAFA

Fly ash used in this study was Class F fly ash (according to ASTM C 618), produced in The Netherlands. The chemical composition, loss on ignition, surface area and mean particle size of fly ash are given in Table 1. The chemical composition of fly ash was determined by X-ray fluorescence spectrometry (XRF). The loss on ignition of the fly ash was determined according to ASTM D 7348-08. The surface area was measured by BET-nitrogen adsorption method and the mean particle size was determined by a Laser diffraction particle size analyzer.

^{*} Corresponding author. Tel.: +86 2039337975. E-mail address: yuwei.ma@hotmail.com (Y. Ma).

Table 1Chemical composition and physical properties of the fly ash used in this study.

Oxide	SiO ₂	Al ₂ O ₃	Fe ₂ O ₃	CaO	MgO	K ₂ O	Na ₂ O	TiO ₂	P ₂ O ₅	SO ₃	L.I.
Weight (%)	48.36	31.36	4.44	7.14	1.35	1.64	0.72	1.24	1.90	1.18	4.89
	Mean particle size (μm):			Surface area (m ² /kg):			1600	Density (g/m³):			2.34

L.I. = loss on ignition.

The activating solutions were prepared by mixing sodium hydroxide (analytical grade, >98% purity) with distilled water and sodium silicate solution (Na₂O: 8.25 wt.%, SiO₂: 27.50 wt.%). All activating solutions were prepared one day before the sample preparation. Table 2 presents the detail mixture proportions of the investigated AAFA mixtures and the compressive strength after curing at 40 °C for 7 days [21].

The cement paste used in this study was CEM I 42.5. The w/c ratio was kept constant at 0.4. The chemical composition of the cement, as well as its density and mean particle size are given in Table 3.

2.2. Sample preparation and testing methods for autogenous shrinkage

Similar to Portland cement paste, the autogenous shrinkage of AAFA pastes were measured by using corrugated tube method (according to ASTM C 1698-09 [22]). The corrugated tube mold effectively prevents the moisture loss and minimizes the restraint to volume change during hardening. Compared to another commonly used method, ASTM C 157, which measures the autogenous shrinkage after 24 h of casting, corrugated tube method is able to measure the autogenous shrinkage immediately after casting (in this study, the autogenous shrinkage was measured from the final setting time). Therefore, the shrinkage behavior of samples during the first 24 h can be captured by using the corrugated tube method.

The freshly mixed AAFA paste for the autogenous shrinkage tests was cast into a corrugated tube mold with a length-to-diameter ratio of approximately 420:29 mm on a vibrating table. The mold was then sealed with plugs and stored at a constant temperature of 40 °C in an oven (the elevated temperature curing is normally needed for AAFA). The length change of the corrugated tube was measured at room temperature by using the length measuring gauge with a measuring accuracy of about 6 $\mu m/m$ [23]. After each measurement, the samples were kept in the oven again. The length change was recorded up to 28 days. Three replicates were measured for each mixture. The first measurement was started at the final setting time (determined by Vicat needle test) of the AAFA pastes. The final setting time of the mixtures 1.0–1.0, 1.0–1.5 and 1.5–1.5 was 2.5 h, 6.0 h and 9.25 h, respectively [24].

2.3. Sample preparation and testing methods for drying shrinkage

The specimens were cast in a mold with the dimensions of $40 \times 40 \times 160$ mm and cured in a sealed condition (with plastic film) at 40 °C. After curing for 7 days, the specimens were exposed in a room with a constant temperature of 20 ± 3 °C and relative humidity of $50\% \pm 5\%$. The length and mass changes of AAFA specimens were monitored by using a comparator with a measuring accuracy of

Table 2Mixture proportion of AAFA mixtures.

Sample (SiO ₂ -Na ₂ O)	Fly ash (g)	SiO ₂ (mol)	Na ₂ O (mol)	H ₂ O (g)	Compressive strength (MPa) ^a
1.0-1.0	1000	1.0	1.0	350	34
1.0-1.5	1000	1.0	1.5	350	45
1.5-1.5	1000	1.5	1.5	350	52

^a Curing at 40 °C for 7 days [21].

Table 3Chemical composition and physical properties of the cement used in this study.

Oxide	CaO	SiO_2	Al_2O_3	Fe_2O_3	MgO	K_2O	Na ₂ O	SO_3
Weight (%) Mean particle		19.5 n):	5.6 16.56	2.3 Density	1.1 (g/m ³):	0.9	0.3 3.15	1.18

0.001 mm and a balance with an accuracy of 0.01 g, respectively. For comparison, the drying shrinkage of cement paste (CEM I 42.5) with a w/c ratio of 0.4 was also measured. The measurements for cement paste started after sealed curing at 20 $^{\circ}\text{C}$ for 7 days. At least two replicates were measured for each mixture.

2.4. Ellipse ring test: cracking of sealed specimens

The ellipse ring test is a simple and fast way to assess the cracking potential of the material under the restrained condition at early ages. Compared to a circular shape, an elliptical shape can generate a higher stress concentration [25]. When the sample shrinks (induced by the autogenous shrinkage in this study), the steel ring limits this movement, resulting in the development of tensile stress. If the tensile stress exceeds the tensile strength of the tested sample, cracking will occur. Although the stress state at the location of the crack is not exactly known, the ellipse ring test provides an indication of the cracking tendency of the mixtures by monitoring the appearance of the cracks on the tested samples.

The AAFA pastes were cast in an annular space (with a width of 40 mm) around a steel ellipse ring with a long axis of 560 mm, short axis of 200 mm and height of 80 mm (as shown in Fig. 1). After casting, the specimens for the ellipse ring tests were sealed with plastic film and cured at 40 °C. The samples were checked regularly during the first 7 days of curing to monitor the crack formation on the surface of AAFA samples.

2.5. Internal relative humidity

The internal RH development of AAFA pastes was measured by Rotronic HygroLab C1 equipped with two HC2-AW RH station probes with an accuracy of $\pm\,1\%$ RH. Prior to the tests, the RH probes were placed in a temperature controlled chamber at 40 $\pm\,1\,^{\circ}$ C for 24 h, and then calibrated by using saturated salt solutions with a known constant RH in the range of 65–95%. After the calibration, the freshly mixed AAFA pastes were cast in two plastic containers and put into the measuring chambers. The RH in the samples and the temperature were recorded every 1 minute for about 3 days. Two replicates were measured for each mixture.

2.6. Evaporable and non-evaporable water content

Both the evaporable and non-evaporable water contents in AAFA pastes were measured in this study. The categorization of water in evaporable and non-evaporable for AAFA pastes is similar to that used for cement-based materials proposed by Powers and Brownyard [26]. The evaporable water content was determined by measuring the weight loss per gram of the sample after heating it to a constant weight at 105 °C. The non-evaporable water content was determined by measuring the weight loss per gram of the sample between 105 °C and 950 °C. The evaporable ($W_{\rm e}$) and non-evaporable ($W_{\rm ne}$) water contents were calculated according to the following equations:

$$We = \frac{W0 - W1}{W0} \tag{1}$$

$$Wne = \frac{W_1 - W_2}{W_2} - L\alpha \tag{2}$$

Download English Version:

https://daneshyari.com/en/article/1456236

Download Persian Version:

https://daneshyari.com/article/1456236

<u>Daneshyari.com</u>